# Fine structure of the local pseudogap and Fano scattering near zigzag graphene edges

Grigory Tkachov
*Max Planck Institute for the Physics of Complex Systems, 01187 Dresden, Germany*

An interplay of evanescent and extended quasiparticle states in the local density of states (LDOS) of zigzag-terminated graphene is investigated using the Green's function of the Dirac equation. The evanescent (edge) states result in a zero-energy peak in the LDOS whose intensity fades out with distance from the edge as $d^{-2}$, revealing an oscillatory contribution of the standing Dirac waves with a slower $d^{-1/2}$ decay. Similar structures, superimposed on the linear pseudogap, were recently observed in STM experiments. The paper also discusses Fano resonant scattering due to the graphene edge states, in close analogy to the phenomenon observed in semiconductor quantum-dot structures. The Fano resonance is found to have a profound effect on transport of both normal and superconducting electrons in contacts with zigzag-terminated graphene.

PACS numbers: 73.23.Ad,74.50.+r,74.78.Na

Experimental evidence[1,2] for massless Dirac-like quasiparticles in graphene - a carbon monolayer with the hexagonal structure - has stimulated vigorous interest in electronic properties of this system (e.g. Refs. 3–11). The unit cell of graphene contains two atoms each belonging to a triangular sublattice, and the low-energy states are described by a two-dimensional Dirac equation where the role of spin is assumed by the sublattice degree of freedom (pseudospin)[12,13]. By analogy with relativistic spin-half particles in two dimensions, the graphene bulk density of states has a linear pseudogap around zero energy $E = 0$ (Ref. 1). Natural boundaries of graphene can however give rise to additional spectral features such as the low-energy branches of edge states[14–17] that are unique to low-dimensional carbon. These states are localized near zigzag-shaped edges, whose outmost atoms all belong to the same sublattice, and originate from the effective pseudospin "polarization" due to vanishing of one of the pseudospinor components as required by particle conservation[5]. The energies of the edge states merge with the Fermi level, producing a peak on top of the pseudogap[14,15] observed in recent scanning tunneling microscope (STM) measurements of the local density of states (LDOS) near zigzag graphene edges[16,17].

The measurements[16,17] also revealed a fine oscillatory structure superimposed on the linear pseudogap with an amplitude increasing with energy[17]. On the other hand, numerical simulations of Ref. 18 found damped oscillations in the LDOS as a function of the position from the edge. A physical picture reconciling the two types of oscillatory phenomena has not yet emerged. The present study interprets both findings as a signature of standing Dirac electron waves near graphene edges. To demonstrate this point, the one-particle Green's function of the Dirac equation was calculated for clean graphene with a zigzag edge described by the boundary condition of Ref. 5. Then, the following expression for the LDOS $\nu(E,d)$, as a function of energy $E$ and distance $d$ from the edge, was obtained

$$\nu(E,d) = |E|\frac{1+J_0\left(\frac{2Ed}{\hbar v}\right)}{\pi(2\hbar v)^2} - \frac{J_1\left(\frac{2|E|d}{\hbar v}\right)}{4\pi\hbar v d} + \frac{\delta(E)}{4\pi d^2}. \quad (1)$$

Here the delta-functional term results from the dispersionless zero-energy edge state whereas the oscillating component given by the Bessel functions $J_0(2Ed/\hbar v)$ and $J_1(2|E|d/\hbar v)$ is due to the standing waves formed of the states belonging to the Dirac spectrum ($v$ and $\hbar$ are the electron velocity and Plack's constant). Similar to the experiments of Refs. 16,17, with increasing $d$ the edge-state contribution gets suppressed while an oscillatory pattern emerges on top of the linear pseudogap (see, also Fig. 1(a)). Its period is inversely proportional to $d$ and the amplitude increases with energy as $\sqrt{|E|}$. At the same time, the spatial dependence of the LDOS shown in Fig. 1(b) agrees with the numerical simulations of Ref. 18.

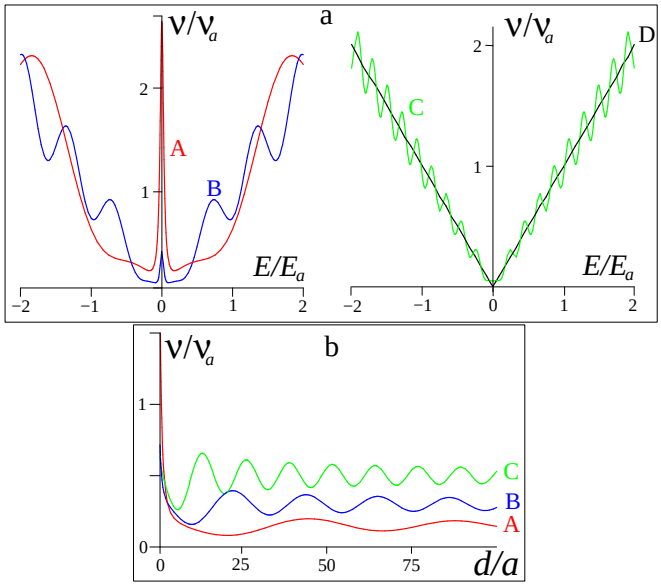


FIG. 1: (a) LDOS vs. energy at different distances from the edge: (A) $d = 4a$, (B) $d = 10a$, (C) $d = 30a$, (D) $d = 10000a$; where $a = 0.246\,\mathrm{nm}$ is graphene's lattice constant, $\nu_a = 1/8\pi\hbar v a$ and $E_a = \hbar v/2a$. (b) LDOS vs. distance from the edge for different energies: (A) $E = 0.15E_a$, (B) $E = 0.3E_a$, (C) $E = 0.5E_a$. The delta function in Eq. (1) is approximated by a Lorenzian $o/\pi(E^2+o^2)$ with $o = 0.03E_a$.

Section I of the present article containes the details of the calculation of the LDOS.

We notice that the spectral contribution of the edge state in Eq.(1) resembles that of a discrete quantum level with energy $E = 0$. One may therefore expect that zigzag graphene edges contacted by conventional conductors would exhibit certain properties of quantum dots. The Green's function approach adopted here allows us to investigate such a possibility as well. It is done for a model system where a quasi-one-dimensional conducting channel is side-coupled to a zigzag graphene edge via a tunnel barrier. In the equilibrium case, the Fermi levels in the two systems are aligned and, hence, the graphene edge state acts as a resonant level $E = 0$ destructively interfering with the continuum states in the channel. The channel transmission is found to vanish at $E = 0$ resonantly, similar to a well-known phenomenon of the Fano resonance[19] (see, section II). Recently, Fano scattering has been observed in ballistic semiconductor channels side-coupled to electrostatically defined quantum dots (e.g. Refs. 20–22). The present work points to a possibility of Fano scattering without the actual quantum-dot electron confinement, which in practical terms could be advantageous. From the theoretical point of view, the hybrid system considered here is suitable for studying the influence of the Dirac electron edge states on transport of correlated electrons. Section III of the article discusses an anomalous Josephson effect due to the Fano scattering of superconducting electrons. Surprisingly, it turns out that the critical Josephson current reaches its maximum at finite temperatures. For a spin-split edge state, spin-dependent Fano scattering causes $0 - \pi$ transitions similar to those in ferromagnetic Josephson junctions[23–28]. In the context of the Josephson effect in graphene (e.g. Refs. 29,30) these issues have not yet been addressed.

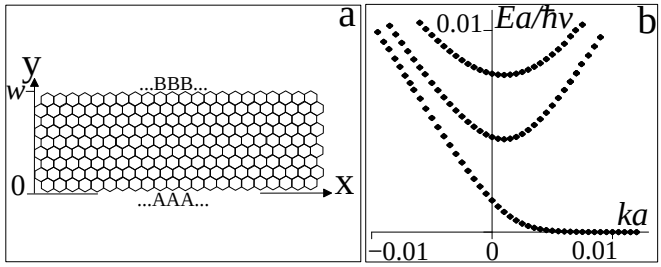


FIG. 2: (a) Schematic view of a zigzag-edge graphene ribbon of width $w$. (b) Quasiparticle spectrum for ribbon's width $w = 1000a$. The flat portion of the lowest subband corresponds to the electron edge state. The spectrum is symmetric with respect to the Fermi level $E = 0$.

## I. GREEN'S FUNCTION OF A ZIGZAG GRAPHENE RIBBON

We consider a graphene strip terminated at $y = 0$ and $y = w$ by atomic lines belonging to different sublattices, conventionally denoted as A and B [Fig. 2(a)]. In the absence of scattering between the two valleys, $K$ and $K'$, of graphene's Brillouin zone[13] we only need to calculate the Green's function in one of them, e.g. $K$, where the Dirac equation reads

$$[\sigma_0 E + i\hbar v(\sigma_x \partial_x + \sigma_y \partial_y)]G = \sigma_0 \delta(x - x')\delta(y - y'). \quad (2)$$

Here the (retarded) Green's function matrix

$$G = \begin{pmatrix} G_{AA} & G_{AB} \\ G_{BA} & G_{BB} \end{pmatrix},$$

Pauli $\sigma_{x,y}$ and unity $\sigma_0$ matrices all act in pseudospin space. It is sufficient to solve the pair of coupled equations for $G_{AA}$ and $G_{BA}$. After expanding in plane waves $\mathrm{e}^{ikx}$, the equations for the Fourier components $G_{AA|k}$ and $G_{BA|k}$ can be reduced to

$$G_{BA|k} = (\hbar v/E)(k + \partial_y)G_{AA|k}, \quad (3)$$

$$[\partial_y^2 - q^2]G_{AA|k} = (E/\hbar^2 v^2)\delta(y - y'), \quad (4)$$

with $q^2 = k^2 - (E/\hbar v)^2$. We seek the solution to Eq. (4) in the form

$$G_{AA|k}(y, y') = a(y')\mathrm{e}^{-qy} + b(y')\mathrm{e}^{qy} - E\mathrm{e}^{-q|y-y'|}/2\hbar^2 v^2 q,$$

where the last term is the Green's function of an unbounded system, and the coefficients $a(y')$ and $b(y')$ are to be found from the boundary conditions $G_{BA|k}|_{y=0} = (k + \partial_y)G_{AA|k}|_{y=0} = 0$ and $G_{AA|k}|_{y=w} = 0$ suggested in Ref. 5 for zigzag ribbons. Finally, we arrive at the following result

$$G_{AA|k}(y, y') = \frac{E}{2\hbar^2 v^2 q} \times$$
$$\times \left\{ \frac{k[\cosh q(w - |y - y'|) - \cosh q(w - y - y')]}{q\cosh qw - k\sinh qw} - \right.$$
$$\left. - \frac{q[\sinh q(w - |y - y'|) + \sinh q(w - y - y')]}{q\cosh qw - k\sinh qw} \right\}. \quad (5)$$

The poles of $G_{AA|k}$, given by the equation $q = k\tanh qw$ (cf. Ref. 5), determine the excitation spectrum shown in Fig. 2(b) for an approximately 250 nm-wide strip. For $k > 0$ the lowest energy subband has an almost flat branch merging with the Fermi level $E = 0$, first found in the tight-binding calculations of Ref. 14. In real space, this branch corresponds to the exponentially decaying $G_{AA|k}(y, y')$ from the edge $y = 0$ into the interior. For wide enough ribbons one can simplify the expression for the Green's function (5) by taking the limit $w \to \infty$:

$$G_{AA|k}(y, y') = -\frac{E\mathrm{e}^{-q|y-y'|}}{2\hbar^2 v^2 q} + \frac{(q + k)^2 \mathrm{e}^{-q(y+y')}}{2qE}. \quad (6)$$

It is instructive to examine Eq. (6) near zero energy,

$$G_{AA|k}(y, y') \approx \frac{(|k| + k)^2 \mathrm{e}^{-|k|(y+y')}}{2|k|E}, \quad |E| \to 0. \quad (7)$$

For $k > 0$ it has a pole $E = 0$ corresponding to a dispersionless edge state. Using Eq. (6), we find an exact position representation for the Green's function $G_{AA}(xy, xy') = \int_{-\infty}^{\infty} dk G_{AA|k}(y, y')/(2\pi)$ as

$$G_{AA}(xy, xy') = \frac{EY_0(k_E|y-y'|) - i|E|J_0(k_E|y-y'|)}{(2\hbar v)^2} + \frac{EY_0(k_E(y+y')) - i|E|J_0(k_E(y+y'))}{(2\hbar v)^2} - \frac{2EY_1(k_E(y+y')) - 2i|E|J_1(k_E(y+y'))}{(2\hbar v)^2 k_E(y+y')}, \quad (8)$$

where $J_n(z)$ and $Y_n(z)$ $(n = 0, 1)$ are, respectively, the Bessel and Neumann functions, and $k_E = \sqrt{E^2}/\hbar v$. To obtain the expression for the LDOS [Eq. (1)] we use $\nu(E, d) = -(1/\pi)\mathrm{Im}G_{AA}(xy, xy')|_{y=y'=d}$, accounting for the pole of the function $Y_1(z) = -2/\pi z + ...$ that corresponds to the zero-energy edge state.

Near the edge the energy dependence of the LDOS is dominated by the singular contribution of the zero-energy edge state as shown in Fig. 1(a) (curve A). In the limit $d \to \infty$ the LDOS recovers the linear pseudogap behavior $\nu \propto |E|$ typical of bulk Dirac electrons (black curve D in Fig. 1(a)). However, at finite distances $d \approx 10 - 100a$ the linear increase in $\nu(E)$ is accompanied by oscillations becoming more pronounced at larger energies (curves B and C in Fig. 1(a)). Oscillations of the same origin are also seen in the position dependence of the LDOS shown in Fig. 1(b). They are due to the interference of the Dirac electron waves incident at and reflected from the edge with small momenta $|k| \leq |E|/\hbar v$ [see Eq. (6)]. At low energies the period of the spatial oscillations is much bigger than the lattice constant $a$ (curves A and B in Fig. 1(b)). That is why they can be resolved by the STM tip.

Interestingly, near the edge Green's function (8) assumes a universal form,

$$G_{AA}(xy, xy') \approx 1/\pi E(y+y')^2, \qquad y, y' \to 0, \quad (9)$$

independent of the material parameters. The formal divergence at $y = y' = 0$ is a consequence of the effective continuum description of the electronic states by the Dirac equation. For further use it is convenient to introduce a physical cutoff for the surface value of the Green's function as $G_{AA}(x0, x0) \approx 1/4\pi E d_c^2$ with $d_c \sim a$.

## II. FANO SCATTERING AT A ZIGZAG GRAPHENE EDGE

It is of both fundamental and practical importance to understand the impact of surface electronic properties of graphene on charge transport at interfaces with conventional conductors. Here we consider a model system [Fig. 3] consisting of a quasi-one-dimensional ballistic channel and a zigzag graphene ribbon coupled in parallel via a point-like tunnel barrier described by a real-space tunneling Hamiltonian of the form

$$H_T = \psi_w^\dagger(0)(\mathcal{T}\psi_A(\mathbf{r}_0) + \mathcal{T}'\psi'_A(\mathbf{r}_0)) + \text{h.c.}, \ \mathbf{r}_0 = (0, 0).$$

Here the electron creation operator in the wire, $\psi_w^\dagger(0)$ at the contact point $x = 0$ is coupled to the annihilation operators of Dirac electrons on sublattice A in both valleys $K$, $\psi_A(\mathbf{r}_0)$ and $K'$, $\psi'_A(\mathbf{r}_0)$ with the matrix elements $\mathcal{T}$ and $\mathcal{T}'$.

Electron scattering in the wire can be investigated with the use of a retarded Green's function $G_w(x, x')$. For the local tunneling Hamiltonian $H_T$, it can be calculated nonperturbatively using the method of the equations of motion, which yields

$$G_w(x, x') = G_w^{(0)}(x, x') + \frac{G_w^{(0)}(x, 0)\Sigma\, G_w^{(0)}(0, x')}{1 - G_w^{(0)}(0, 0)\Sigma}. \quad (10)$$

Here

$$G_w^{(0)}(x, x') = \frac{e^{ik_w|x-x'|}}{i\hbar v_F}, \quad k_w \approx k_F + \frac{E}{\hbar v_F}, \quad (11)$$

is the Green's function in the absence of tunneling ($v_F$ and $k_F$ are the Fermi velocity and wave number in the channel), and the tunneling self-energy is

$$\Sigma = |\mathcal{T}|^2 G_{AA}(\mathbf{r}_0, \mathbf{r}_0) + |\mathcal{T}'|^2 G'_{AA}(\mathbf{r}_0, \mathbf{r}_0). \quad (12)$$

In our case the Green's function $G'_{AA}(\mathbf{r}_0, \mathbf{r}_0)$ in valley $K'$ coincides with $G_{AA}(\mathbf{r}_0, \mathbf{r}_0)$ given by Eq. (9). Using Eqs. (9) and (10)–(12) we find the LDOS $\nu_w(E) = -\mathrm{Im}G_w(0, 0)/\pi$ at the contact point and the transmission amplitude $t = i\hbar v_F G_w\left(\frac{L}{2}, -\frac{L}{2}\right)$ between the reservoirs[31] as follows

$$\nu_w(E) = \frac{1}{\pi\hbar v_F}\frac{E^2}{E^2 + \Gamma^2}, \quad t(E) = \frac{E}{E + i\Gamma}e^{ik_w L}, \quad (13)$$

where the energy $\Gamma = (|\mathcal{T}|^2 + |\mathcal{T}'|^2)/4\pi d_c^2 \hbar v_F$ determines the tunneling rate $\Gamma/\hbar$ between the systems.

We note that the pole of the Green's function (9) results in the zero of both the LDOS and the transmission

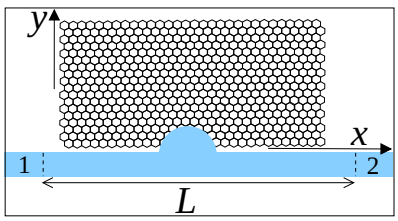


FIG. 3: Schematic view of a zigzag-edge graphene ribbon with a side tunnel contact to a quasi-one-dimensional conducting wire connecting electron reservoirs 1 and 2. The contact is assumed point-like, that is its size is much bigger than the interatomic distances, but smaller than the electronic mean free paths in both wire and graphene.

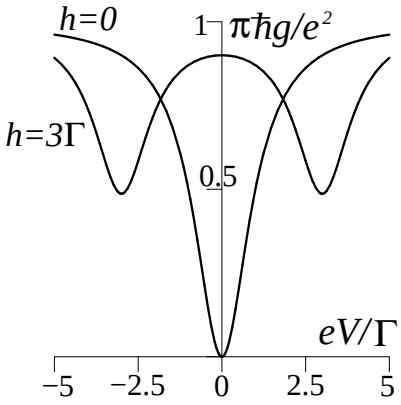


FIG. 4: Zero-temperature conductance $g$ vs. bias voltage $V$ for spin-degenerate ($h = 0$) and spin-split ($h = 3\Gamma$) edge state in graphene. In the latter case the two minima manifest the spin-filtering effect when the contribution of one of the spin species resonantly vanishes.

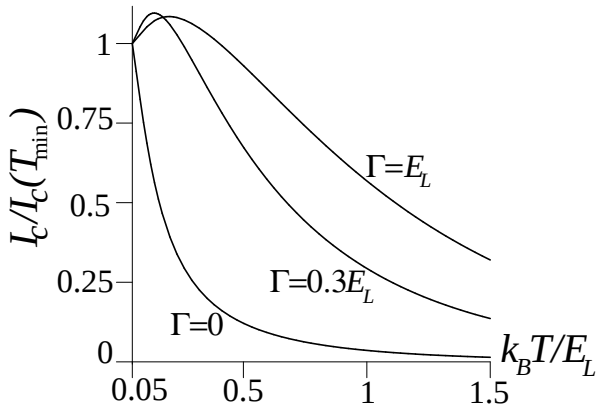


FIG. 5: Critical current vs. temperature for a spin-degenerate edge state: $h = 0$, $\gamma = 0.1E_L$, $\Delta = 10E_L$. The current is normalized to the value $I_c(T_{min})$ where $T_{min} = 0.05E_L/k_B$ is the lowest temperature for which the condition $\gamma \le \pi k_B T \ll \Delta$ of weak proximity effect still holds.

amplitude (13) at $E = 0$, manifesting complete backscattering of an electron wave incoming from one of the reservoirs. The Fano-like transmission antiresonance at $E = 0$ is due to destructive interference between the electron wave directly transmitted through the wire (without tunneling) and the wave transmitted via tunneling through the graphene edge state whose energy is pinned to the Fermi level in the wire. A peculiar feature of this transmission antiresonance is that its width $\Gamma$ does not depend on the electron velocity $v$ in graphene.

It is straightforward to generalize our analysis to a spin-split edge state in graphene with energies $\mp h$ for spin projections $\alpha = \pm 1/2$. In this case, equation (13) for $t(E)$ transforms to

$$t_\alpha(E) = \frac{E + 2\alpha h}{E + 2\alpha h + i\Gamma} e^{ik_w L}. \qquad (14)$$

Below we briefly discuss the dependence of the zero-temperature Landauer conductance $g(V) = e^2/(2\pi\hbar)\sum_{\alpha=\pm 1/2} |t_\alpha(eV)|^2$ on the bias voltage $V$. As shown in Fig. 4, the conductance is suppressed at $V = 0$ for the spin-degenerate edge state, whereas for $h = 3\Gamma$ the conductance dip is spin-split and the minima manifest the spin-filtering effect when the contribution of one of the spin species resonantly vanishes. Such effect was earlier discussed for side-coupled quantum dots[32,33] in the context of possible applications in spintronics[34].

## III. FANO SCATTERING OF SUPERCONDUCTING ELECTRONS

We turn now to the case of superconducting reservoirs supporting an equilibrium Josephson current. The Josephson coupling is maintained due to the Andreev process[35] whereby an electron is retro-reflected as a Fermi-sea hole from one of the superconductors with the subsequent hole-to-electron conversion in the other one. Such an Andreev reflection circle facilitates a Cooper pair transfer between the superconductors. Naturally, between the Andreev reflection events both the electron and the hole can experience normal scattering inside the junction. That is why the transmission antiresonance discussed above is expected to strongly influence the Josephson current. It is convenient to use the approach of Refs. 36,37 relating the supercurrent to the scattering amplitudes via a sum over the Matsubara frequencies $\omega_n = (2n + 1)\pi k_B T$ as follows

$$I_c = -\frac{4ek_BT}{\hbar} \sum_{n\ge 0,\alpha} \mathrm{a}_\alpha^2(E) t_\alpha(E) t^*_{-\alpha}(-E)|_{E=i\omega_n}. \qquad (15)$$

Here the hole transmission amplitude $t^*_{-\alpha}(-E)$ is related to the electrone one [Eq. (14)] since the hole motion is governed by the time-reversed counterpart of the electron Hamiltonian[36,38], and $\mathrm{a}_\alpha(E)$ is the Andreev reflection amplitude at the point contacts to superconductors 1 and 2. Equation (15) is applicable for arbitrary $t_\alpha(E)$ as long as $\mathrm{a}_\alpha^2$ is small enough so that one can neglect higher order Andreev processes. This is one of the situations where the junction has the sinusoidal current phase relation $I(\varphi) = I_c \sin\varphi$. Equation (15) gives thus the critical value of the current.

To proceed we need to clarify the model for Andreev reflection employed here. In point contacts to conventional Bardeen-Cooper-Schrieffer (BSC) superconductors the amplitude $\mathrm{a}_\alpha$ can be calculated using the scattering approach of Ref. 39. However, in many practical cases superconducting contacts to low-dimensional systems can hardly be regarded as BCS-like ones. Proximity-effect contacts to semiconductor nanowires[44,45] and carbon nanotubes[46,47] are important examples of such a situation. In this case a thin normal-metal layer is inserted between the superconductor and the wire to ensure a good electrical contact. In proximity-effect point contacts the Andreev scattering amplitude can be expressed in terms

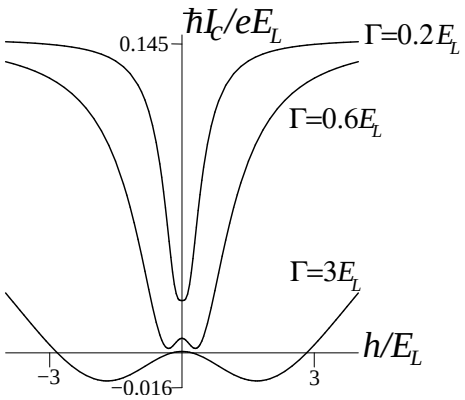


FIG. 6: Critical current vs. spin-splitting energy: $T = 0.1E_L/k_B$, $\gamma = 0.1E_L$, $\Delta = 10E_L$.

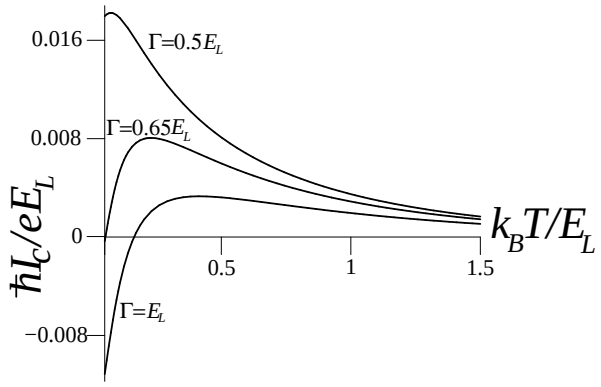


FIG. 7: Critical current vs. temperature for a spin-polarized edge state: $h = 0.5E_L$, $\gamma = 0.1E_L$, $\Delta = 10E_L$.

of the quasiclassical condensate $\mathcal{F}_\alpha(\omega_n)$ and quasiparticle $\mathcal{G}_\alpha(\omega_n)$ Green's functions of the normal layer as follows[40,41]

$$\mathrm{a}_\alpha(\omega_n) = \frac{i\mathcal{F}_\alpha(\omega_n)}{1+\mathcal{G}_\alpha(\omega_n)}. \tag{16}$$

We will adopt this approach and make use of McMillan's expressions[42,43] for the Green's functions:

$$\mathcal{F}_\alpha = \frac{\Delta_n}{\sqrt{\omega_n^2+\Delta_n^2}},\ \mathcal{G}_\alpha = \frac{\omega_n}{\sqrt{\omega_n^2+\Delta_n^2}}, \tag{17}$$

$$\Delta_n = \frac{\gamma\Delta}{\gamma+\sqrt{\omega_n^2+\Delta^2}}, \tag{18}$$

where $\Delta$ is the pairing energy in the superconductor. McMillan's parameter $\gamma$ characterizes the deviation of the Green's functions from the BCS form which is recovered for $\gamma \gg \Delta$. Physically, it controls the strength of the proximity effect in the normal layer and, therefore, the Andreev reflection amplitude $\mathrm{a}_\alpha(\omega_n) = i\Delta_n/(\omega_n + \sqrt{\omega_n^2+\Delta_n^2})$. For a weak proximity effect with $\gamma \le \pi k_B T \ll \Delta$, the amplitude $\mathrm{a}_\alpha^2$ is small[48] and we can use Eq. (15) which can be rewritten as

$$I_c = \frac{8ek_BT}{\hbar}\sum_{n\ge 0}\frac{\Delta_n^2 \mathrm{e}^{-\omega_n/E_L}}{[\omega_n+\sqrt{\omega_n^2+\Delta_n^2}]^2}\mathrm{Re}\frac{(h+i\omega_n)^2}{[h+i(\omega_n+\Gamma)]^2}, \tag{19}$$

where the exponential factor results from the dynamical phase $2EL/\hbar v_F$ accumulated in the Andreev circle, introducing the Thouless energy $E_L = \hbar v_F/2L$. It is used below as an energy unit.

Figure 5 shows the temperature dependence of the critical current (19) for the spin-degenerate case ($h = 0$). In the absence of tunneling ($\Gamma = 0$) it is just a monotonic exponential decrease. However, for $\Gamma \neq 0$ the interplay of the transmission antiresonance and the exponential suppression gives rise to a maximum at finite temperatures.

Spin splitting of the graphene edge state lifts the Fano resonance condition $E = 0$ for both electron and Andreev reflected hole. Therefore, for relatively weak tunneling coupling, under conditions $\pi k_B T \le \Gamma < E_L$, the critical current increases with $h$ (see, Fig. 6), a behavior quite unusual for Josephson junctions. Surprisingly, for stronger tunneling coupling ($\Gamma > E_L$) the function $I_c(h)$ becomes nonmonotonic with a rather broad region $h_1 \le |h| \le h_2 \approx \Gamma$ where $I_c$ is negative [Fig. 6]. The lower boundary $h_1 \approx \pi k_B T$ is set by the temperature and is much smaller than all $E_L$, $\Gamma$ and $\Delta$. This can be proven analytically by expanding Eq. (19) under conditions $h, \pi k_B T < E_L \ll \Gamma$ as follows

$$I_c = \frac{8ek_BT}{\hbar}\sum_{n\ge 0}\frac{\Delta_n^2 \mathrm{e}^{-\omega_n/E_L}}{[\omega_n+\sqrt{\omega_n^2+\Delta_n^2}]^2}\frac{\omega_n^2-h^2}{\Gamma^2}. \tag{20}$$

The supercurrent reversal is a consequence of the spin-dependent phases acquired by both electron and hole due to scattering off the spin-polarized graphene edge. Negative values of $I_c$ imply a built-in $\pi$ phase difference in the ground state of a Josephson junction as opposed to $\varphi = 0$ for positive $I_c$[49]. This so-called $\pi$ state is known to occur in superconductor/ferromagnetic/superconductor junctions where the condensate function in the ferromagnet oscillates in space[23–26] (see, also recent reviews 27,28). The author is not aware of any earlier work predicting $0-\pi$ transitions due to spin-dependent Fano scattering. Figure 7 also shows that for the spin-polarized graphene the $0-\pi$ transition can be driven by temperature with an averall strongly nonmonotonic dependence of $I_c(T)$.

## IV. SUMMARY

In the present work, electronic states near zigzag graphene edges have been investigated using the Green's function of the Dirac equation. This approach adequately describes the states localized at the zigzag edge and their contribution to the local density of states (LDOS) studied earlier theoretically[14,15] and experimentally[16,17]. On an equal footing, it accounts for the contribution of the standing Dirac waves that turns out to be an oscillating function of both energy and distance from the edge. Similar oscillatory pattern in the tunneling conductance

was observed in the STM measurements of Refs. 16,17, although its origin was not identified previously. Since the oscillating component discussed here is not related to the edge states, it is expected to occur for other edge geometries, e.g. for the armchair edge. This conclusion also agrees with the experiments of Refs. 16,17. In practice, the oscillations of the LDOS due to the formation of standing waves could serve as a means of controlling the quality of graphene samples.

Another issue this study has addressed is the influence of the Dirac electron edge states on electron transport. Fano scattering has been predicted in a ballistic conductor side-coupled to a zigzag graphene edge. It has been also shown that the Fano resonance can result in a variety of unusual behaviors of the Josephson critical current. Going back to the role of the spin splitting of the graphene edge state, it is worth mentioning that the most interesting effects occur for weak spin-splitting energy around $h = 0$ [see, Fig. 6] where it competes with the thermal energy $\pi k_B T$ only. One may therefore expect that in the millikelvin range such a spin splitting could be induced by a rather weak external magnetic field. The issue of the edge states and their effect on electron transport in carbon nanostructures is of current theoretical interest motivated by potential applications in nanoelectronics (see, e.g. Ref. 50).

The author thanks G. Cuniberti, M. Hentschel and C. Strunk for discussions. This work was partially funded by the European Union grant CARDEQ under Contract No. FP6-IST-021285-2.


[1] K. S. Novoselov, A. K. Geim, S. V. Morozov, D. Jiang, M. I. Katsnelson, I. V. Grigorieva, S. V. Dubonos, and A. A. Firsov, Nature (London) **438**, 197 (2005).

[2] Y. Zhang, Y.-W. Tan, H. L. Stormer, and P. Kim, Nature (London) **438**, 201 (2005).

[3] V. P. Gusynin and S. G. Sharapov, Phys. Rev. Lett. **95**, 146801 (2005).

[4] N. M. R. Peres, F. Guinea, and A. H. Castro Neto, Phys. Rev. B **73**, 125411 (2006).

[5] L. Brey and H. A. Fertig, Phys. Rev. B **73**, 235411 (2006).

[6] E. McCann and V. I. Falko, Phys. Rev. Lett. **96**, 086805 (2006).

[7] K. Nomura and A. H. MacDonald, Phys. Rev. Lett. **96**, 256602 (2006).

[8] I. L. Aleiner and K. B. Efetov, Phys. Rev. Lett. **97**, 236801 (2006).

[9] J. Tworzydlo, B. Trauzettel, M. Titov, A. Rycerz, and C. W. J. Beenakker, Phys. Rev. Lett. **96**, 246802 (2006).

[10] C. W. J. Beenakker, Phys. Rev. Lett. 97, 067007 (2006).

[11] V.V. Cheianov, V. Fal'ko, B. L. Altshuler, Science **315**, 1252 (2007).

[12] D. P. DiVincenzo and E. J. Mele, Phys. Rev. B **29**, 1685 (1984).

[13] T. Ando, J. Phys. Soc. Jpn. **74**, 777 (2005).

[14] M. Fujita, K. Wakabayashi, K. Nakada, and K. Kusakabe, J. Phys. Soc. Jpn. **65**, 1920 (1996); K. Nakada, M. Fujita, G. Dresselhaus, and M. S. Dresselhaus, Phys. Rev. B **54**, 17954 (1996).

[15] K. Wakabayashi, M. Fujita, H. Ajiki, and M. Sigrist, Phys. Rev. B **59**, 8271 (1999).

[16] Y. Kobayashi, K. I. Fukui, T. Enoki, K. Kusakabe, and Y. Kaburagi, Phys. Rev. B **71**, 193406 (2005).

[17] Y. Niimi, T. Matsui, H. Kambara, K. Tagami, M. Tsukada, and H. Fukuyama, Phys. Rev. B **73**, 085421 (2006).

[18] Y. Kobayashi, K. I. Fukui, T. Enoki, and K. Kusakabe, Phys. Rev. B **73**, 125415 (2006).

[19] U. Fano, Phys. Rev. **124**, 1866 (1961).

[20] K. Kobayashi, H. Aikawa, S. Katsumoto, and Y. Iye, Phys. Rev. Lett. **88**, 256806 (2002).

[21] A. C. Johnson, C. M. Marcus, M. P. Hanson, and A. C. Gossard, Phys. Rev. Lett. **93**, 106803 (2004).

[22] A. Fuhrer, P. Brusheim, T. Ihn, M. Sigrist, K. Ensslin, W. Wegscheider, and M. Bichler, Phys. Rev. B **73**, 205326 (2006).

[23] A. I. Buzdin, L. N. Bulaevskii, and S. V. Panyukov, JETP Lett. **35**, 178 (1982) [Pis'ma Zh. Eksp. Teor. Fiz. **35**, 147 (1982)].

[24] V. V. Ryazanov, V. A. Oboznov, A. Yu. Rusanov, A. V. Veretennikov, A. A. Golubov, and J. Aarts, Phys. Rev. Lett. **86**, 2427 (2001).

[25] T. Kontos, M. Aprili, J. Lesueur, and X. Grison, Phys. Rev. Lett. **86**, 304 (2001).

[26] A. Bauer, J. Bentner, M. Aprili, M. L. Della Rocca, M. Reinwald, W. Wegscheider, and C. Strunk, Phys. Rev. Lett. **92**, 217001 (2004).

[27] A. A. Golubov, M. Yu. Kupriyanov, and E. Il'ichev, Rev. Mod. Phys. **76**, 411 (2004).

[28] A. I. Buzdin, Rev. Mod. Phys. **77**, 935 (2005).

[29] M. Titov and C. W. J. Beenakker, Phys. Rev. B **74**, 041401(R) (2006).

[30] Ali G. Moghaddam and Malek Zareyan, Phys. Rev. B **74**, 241403(R) (2006).

[31] D. S. Fisher and P. A. Lee, Phys. Rev. B **23**, 6851 (1981).

[32] M. E. Torio, K. Hallberg, S. Flach, A. E. Miroshnichenko, and M. Titov, Eur. Phys. J. B **37**, 399 (2004).

[33] M. Lee and C. Bruder, Phys. Rev. B **73**, 085315 (2006).

[34] I. Žutić, J. Fabian, and S. Das Sarma, Rev. Mod. Phys. **76**, 323 (2004).

[35] A.F. Andreev, Zh. Eksp. Teor. Fiz. **46**, 1823 (1964) [Sov. Phys. JETP **19**, 1228 (1964)].

[36] C.W.J. Beenakker, Phys. Rev. Lett. **67**, 3836 (1991); in *Transport Phenomena in Mesoscopic Systems*, edited by H. Fukuyama and T. Ando, p. 235 (Springer, Berlin 1992).

[37] P.W. Brouwer and C.W.J. Beenakker, Chaos, Solitons and Fractals **8**, 1249 (1997).

[38] P.G. de Gennes, Rev. Mod. Phys **36**, 225 (1964).

[39] G.E. Blonder, M. Tinkham, and T.M. Klapwijk, Phys. Rev. B **25**, 4515 (1982).

[40] A.A. Golubov and M.Yu. Kupriyanov, Physica C **259**, 27 (1996).

[41] A. F. Volkov and A. V. Zaitsev, Phys. Rev. B **53**, 9267 (1996).

[42] W. L. McMillan, Phys. Rev. **175**, 537 (1968).

[43] A. A. Golubov, E. P. Houwman, J. G. Gijsbertsen, V. M. Krasnov, J. Flokstra, H. Rogalla, and M. Yu. Kupriyanov, Phys. Rev. B **51**, 1073 (1995).

[44] J. A. van Dam, Y. V. Nazarov, E. P. A. M. Bakkers, S. De Franceschi, L. P. Kouwenhoven, Nature 442, 667 (2006).
[45] Jie Xiang, A. Vidan, M. Tinkham, R. M. Westervelt and Charles M. Lieber, Nature Nanotechnology 1, 208 (2006).
[46] H.I. Jorgensen, K. Grove-Rasmussen, T. Novotny, K. Flensberg, and P.E. Lindelof, Phys. Rev. Lett. **96**, 207003 (2006).
[47] T. Tsuneta, L. Lechner, and P. J. Hakonen, Phys. Rev. Lett. **98**, 087002 (2007).
[48] G. Tkachov and K. Richter, Phys. Rev. B **75**, 134517 (2007), discusses magnetic pair breaking as a means of controlling the Andreev amplitude in quantum dot Josephson junctions.
[49] L. N. Bulaevskii, V. V. Kuzii, and A. A. Sobyanin, Pis'ma Zh. Eksp. Teor. fiz. **25**, 314 (1977) [JETP Lett. **25**, 290 (1977)].
[50] M. del Valle, R. Gutierrez, C. Tejedor, and G. Cuniberti, Nature Nanotechnology **2**, 176 (2007).